Powder Technology 449 (2025) 120413

Contents lists available at ScienceDirect

Powder Technology

journal homepage: www.journals.elsevier.com/powder-technology

# Design and optimization of stirrer and mixer design for the correct mixing of pharmaceutical powders through DEM

Nizar Salloum [a,b,*], Thomas Brinz [b], Aitor Atxutegi [a], Stefan Heinrich [a]

[a] Institute of Solids Process Engineering and Particle Technology, Hamburg University of Technology, Denickestr. 15, 21073 Hamburg, Germany
[b] Syntegon Technology GmbH, Stuttgarter Str. 130, 71332 Waiblingen, Germany

## HIGHLIGHTS

- Development of a numerical method for quantifying the mixing quality was shown to be robust.
- UV/Vis Spectroscopy was used to validate the numerical results.
- Adding one deflector to the mixer can lead to a significant influence on the powder behavior.
- Using different rotational speeds within the single mixing process can be more advantageous than using a unique speed scheme.
- Correlations between the boundary conditions and material properties should be considered to get the best mixing degree.

## GRAPHICAL ABSTRACT

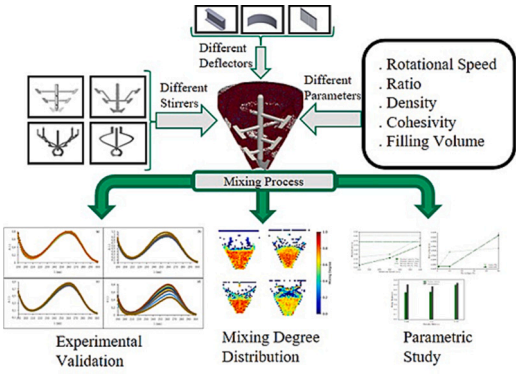


## ARTICLE INFO

*Keywords:*
Discrete element method
Particle mixing
Mixing degree
Mixer design
Calibration

## ABSTRACT

Mixing of granular materials is an important process for pharmaceutical industries. In this study, a quantifiable calculation method was suggested to determine the final mixing degree of the mixture. Based on that, the effect of the stirrer design, rotational speed, powder density, cohesivity, material ratios, and particle movement in the chamber guided through different designs of deflectors on the final mixing quality is examined. The results show that increasing the stirring speed, generates better mixing quality. However, introducing a varying rotational speed mode improves the mixing degree specially for binary mixtures with high relative densities. The improvement of the mixing with the number of contacting blades is observed. Finally, the introduction of a simple deflector drastically enhances the mixing quality and enables the feeding into the chamber, which is key for continuous operation with cohesive powders, making the process more stable and efficient by using more of the mixing volume.

* Corresponding author at: Institute of Solids Process Engineering and Particle Technology, Hamburg University of Technology, Denickestr. 15, 21073 Hamburg, Germany.
*E-mail address:* Nizar.salloum@tuhh.de (N. Salloum).

https://doi.org/10.1016/j.powtec.2024.120413
Received 31 July 2024; Received in revised form 27 October 2024; Accepted 29 October 2024
Available online 7 November 2024

## 1. Introduction

The mixing of powders is an essential process in the food and pharmaceutical industries to gurantee a certain final product quality [1,2]. This quality can be represented in terms of taste, quality, flavor, and texture for food products, where these characteristics are affected by mixture homogeneity [3]. However, in the pharmaceutical industry, homogeneity can be considered a more critical parameter since a little irregularity in the excipients per dosage might be threatening to patients [4]. In this context, being aware of the most affecting parameters to the mixing behavior, i.e., particle properties and boundary conditions, is very critical for optimizing the whole process. These parameters can be characterized as particle size, density, shape, moisture content, roughness, and the presence of inter-particle forces [5]. In order to evaluate the powder mixing state, several methodologies were considered, e.g., X-ray microtomography [6], image analysis [7], and traditional sampling [8]. However, these methods have some disadvantages and restrictions. In microtomography, the position of the particles cannot be detected unless the mixing process is terminated. Upon using image analysis, coloring inks are usually involved in order to follow marker particles, which could change the particle surface properties. If the mixing quality of a bulk region is quantified via traditional sampling, the spatial location of the particles may be changed due to the insertion of a sampling probe. Therefore, using an experimental approach to evaluate the mixing quality of powders remains a challenge [9].

In this study Discrete Element Method (DEM) has been used, given that DEM is one of the main approaches to simulate discrete and granular materials [10] and it is able to represent the mixing of powders. Through DEM, not only the movement of the powders can be captured, but also the 3D interactions of the particles. Several mixing techniques have been examined in the literature using DEM such as static mixers [11], tubular [12], screw conveyor-mixers [13,14], rotating drums [15–17,31], V-blenders [18–20], and Nauta blenders [21].

A focused investigation into ribbon mixers reveals that their complex structure complicates the understanding of mixing mechanisms, which have traditionally been identified as convection without precise empirical validation. One notable study utilizes DEM to develop a novel swept volume measurement approach, confirming convective mixing while highlighting blade width as a critical parameter for enhancing mixing efficiency. This research underscores the potential of numerical modeling to optimize ribbon mixer designs and improve powder mixing outcomes. [22]

Additionally, another investigation examines the predictive capabilities of DEM simulations for a laboratory-scale paddle blade mixer during a powder mixing process. In this study, the visco-elasto-plastic frictional adhesive DEM contact model from Thakur et al. (2014) was employed to represent the cohesive behavior of aluminosilicate powder. Model parameters were determined through experimental flow energy measurements using the FT4 powder rheometer. The DEM simulations effectively reproduced the FT4 flow energy of the powder; however, they exhibited only qualitative agreement with the experimental mixing rates for both dry and wet powders, indicating an under-prediction of mixing. This finding suggests that relying solely on flow energy measurements may not adequately optimize the DEM model for powder mixing. [23]

The main purpose of simulating the particle mixing process is to study the factors, which affect the mixing degree and mixing speed [22]. For quantifying the mixing degree numerically, there are different methods explained in the literature. Choa et al. (2017) represented three different mixing indices namely, Lacey, Kramer, and Lacey-Weidenbaum-Bonilla [23]. He exhaustively investigated the efficiency and limitations of each mixing index, suggesting and developing a new index called the Coordinate mixing index. Apart from the conventional mixing index methods, two other ways of quantifying the mixing degrees were also mentioned in literature [22]. The first method to characterize the mixing degree of particles is contact statistics, i.e., by tracking and recording the total number of contacts between different particles through time, and once the total number of contact oscillates in a relatively small range, the particles are assumed to be evenly mixed [24,25]. The second method is the uniform distribution method, i.e., by dividing the particle bed into equal volume voxels (n samples), the number of characteristic particles in each block is tracked and recorded, after which the standard deviation of the *n* sample values is calculated. By observing the standard deviation, a uniform mixing is assumed when the oscillations of this value are reduced [26–28].

The main purpose of this study is to check the influence of different factors in terms of geometry and particle properties on the mixing degree. For this study, the calculation of the mixing degree using the conventional mixing index, e.g. Lacey Index, is not considered based on several factors. First, the Lacey Index has been reported in some cases to exceed a value of 1 [29]. This phenomenon occured when a relatively small cell size is considered in the calculations, indicating sensitivity to cell size in the assessment of mixing degree. This conflicts with our approach where a value of 1 represents the ideal mixing degree. This inconsistency raises questions about the reliability of the Lacey Index in accurately reflecting mixing quality under certain conditions. Additionally, in our simulations, calculating the Lacey Index proved to be more time-consuming, requiring an additional 10 to 15 min per simulation compared to the method we employed. This is largely due to the increased complexity involved in counting and analyzing particle distributions required by the Lacey Index, which adds to the computational load without providing added value for our specific case.On the other hand, the positioning of the particles in the system involved in this study does not allow the use of the two other above mentioned methods. Therefore, a new way of quantifying the mixing degree was developed and used.

## 2. Methodology

In this study, two distinct pharmaceutical powders (MEGGLE Wasserburg GmbH & Co. KG, Germany) were employed. SpheroLac 100 was chosen to represent free-flowing lactose powder, commonly employed in various applications, such as capsule filling, blends, premixes, sachets, and triturations [32]. Conversely, Vitamin C (Ascorbic Acid) was selected as a cohesive Active Pharmaceutical Ingredient (API), recognized for its potent antioxidant properties and widespread usage across cosmetic and pharmaceutical sectors [33]. While it is recognized that pharmaceutical formulations often include other components such as lubricants, glidants, and disintegrants, the objective of this study was to focus specifically on two powders with contrasting material properties—free-flowing and cohesive powders. This focus was deliberately chosen to evaluate the mixing performance of the equipment under controlled conditions, rather than to formulate a final medicinal product at this stage.

### 2.1. Experimental material characterization

#### 2.1.1. Flowability and shear properties

The investigation of the properties of SperoLac 100 was done in our earlier study [34], where the methodologies of indicating the material properties experimentally are explained. For Ascorbic Acid, the same approaches were followed.

In summary, the Carr index (CI) was utilized to evaluate powder flowability, while cohesion (C) and flowing factor ($FF_c$) values were determined through FT4 powder rheometry. The Mohr-Coulomb model facilitated the derivation of ($FF_c$) from major principal stress ($\sigma_1$) and unconfined yield strength ($\sigma_c$), with subsequent insights into static friction coefficients occurring between the particles ($\mu_{s,pp}$) and wall friction angles ($\varphi_w$), which is used to calculate the coefficient of static friction between a particle and wall ($\mu_{s,pw}$). These findings provide a comprehensive understanding of powder behavior, as previously explored in the referenced work. They were considered as the starting

point for the calibration to obtain the DEM parameters. The results of these measurements are summarized in Table 1.

#### 2.1.2. Particle size and shape characterization

Particle shapes were estimated using dynamic image analysis to measure the volume moment mean (D [3,4]), also known as the De Brouckere Mean Diameter. This method identifies the central point (center of gravity) around which the volume/mass distribution rotates, offering an advantage over other particle size calculation methods as it does not require knowledge of the total number of particles. Additionally, the Camsizer XT was employed to approximate the particle shape by analyzing two-dimensional images in terms of the minimum and maximum Feret diameters (Femin and Femax). Femin represents the length of the minor axis, while Femax represents the length of the major axis. The aspect ratio (ASR), defined as the ratio of Femin to Femax, indicates particle elongation, with values closer to 0 corresponding to elongated particles and values closer to 1 indicating more spherical particles.

Furthermore, following the approach of Li et al. [37], we also considered a shape factor called circularity or roundness (Ro), which quantifies how spherical a particle is based on its projected area (A) and the overall perimeter of projection (P) using the formula

$$R_0 = \frac{4 \times \pi \times A}{P^2} \quad (1)$$

For the purposes of our study, we assumed the particles to be spherical, noting that any deviations from this shape can be effectively compensated by adjusting the coefficient of rolling friction.

#### 2.1.3. Density

The bulk density (BD) was determined using the jolting volumeter (Jel STAV II) from J. Engelsmann AG (Germany). A specific mass of powder was placed into a graduated cylinder, and both the volume and mass were measured. This process was repeated five times to ensure accuracy and consistency, with the average value being recorded. The bulk density reflects the average density of the powder sample, taking into account the voids present between individual particles. As a result, the bulk density is influenced by the material density of the particles as well as their spatial arrangement. Additionally, the volume of a bulk solid is affected by the size and shape of its particles.

The particle (true) density ($\rho_p$) was measured using the Ultrapyc 1200e, an automatic density analyzer from Quantachrome Instruments (USA). This device is a pycnometer that assesses the true density of powder samples by employing an inert gas (helium) to determine volume through Archimedes' principle of displacement and the gas expansion method (Boyle's law). Table 2 shows the properties defining the size and the shape of the particles, in addition to the values of densities of both powders.

### 2.2. DEM simulations

DEM simulations were conducted utilizing the open-source software LIGGGHTS®, specifically LIGGGHTS-Premium 4.X. These simulations were executed on an eight-node high-performance cluster located at HLRS Stuttgart, with each node featuring 2 × 12 CPUs (Intel Xeon E5-2680v3 @ 2.50GHz, Haswell architecture) and 128GB of memory. Post-processing of the simulation data was carried out using ParaView version 5.4.1 (64-bit). The three-dimensional CAD models employed in the DEM simulations were created using SolidWorks Premium, while meshing of these models was accomplished using Gmsh version 3.0.6.

**Table 1**
Flowability and shear properties.

| | *CI (%)* | C (kPa) at 6 kPa | ffc at 6 kPa | AIF (°) | $\mu_{s,pp}$ | WFA (°) | $\mu_{s,pw}$ |
|---|---|---|---|---|---|---|---|
| SpheroLac 100 | 10.82 | 0.12 | 20.83 | 31.38 | 0.61 | 6.58 | 0.115 |
| Ascorbic Acid | 31.89 | 0.81 | 3.71 | 28.64 | 0.546 | 5.74 | 0.10 |

**Table 2**
Particle size, shape and bulk properties.

| | *D* [3,4] (μm) | ASR | Ro | BD (kg/m$^3$) | $\rho_p$ (kg/m$^3$) |
|---|---|---|---|---|---|
| SpheroLac 100 | 115 | 0.746 | 0.891 | 758 | 1536.1 |
| Ascorbic Acid | 42 | 0.704 | 0.852 | 523 | 1693.6 |

#### 2.2.1. Contact models and parameters

For the DEM simulations, the Hertz-Mindlin contact model in conjunction with the rolling friction model (EPSD2) was employed, in addition to the adhesion contact model (SJKR) to accurately capture the behavior of the two powders. Parameters such as Young's modulus (Y), Poisson's ratio ($\nu$), and the coefficient of restitution for both the mixer and the stirrer were gleaned from pertinent literature sources. The coefficients of static friction (particle-particle), static friction (particle-wall), and rolling friction (particle-particle) were determined utilizing our previously developed semi-automated DEM parameter calibration technique, as outlined in an earlier study [36]. This technique leverages design of experiment (DoE) principles to streamline experimentation, enabling a precise understanding of parameter influences on material behavior while minimizing the number of trials required. Subsequently, a predictive model was established, facilitating anticipation of material responses to parameter alterations. Finally, through superimposing graphs representing predicted responses based on varying parameter combinations, a unique parameter set that accurately represented the materials was indentified.

#### 2.2.2. Particles scaling-up method

In the perfomed simulations, a single particle size was utilized for each type of powder, with a focus on specific material properties relevant to the study. No particle size distribution was considered, as the objective was to analyze the mixing performance using distinct powder characteristics.The scaling-up strategy followed the coarse-graining (CG) method as proposed by Bierwisch et al. [35]. This approach is designed to balance computational time and accuracy in DEM simulations by limiting the number of particles. In the CG method, original particles with radius R are replaced by larger grains with radius $R' = R \times S_f$, where $S_f$ is the scaling factor. This method adjusts the interaction laws and equations of motion to preserve energy densities—both gravitational potential and kinetic energy—within the scaled-up system.

Importantly, the particle density remains fixed, ensuring that the volume fraction and potential energy are comparable to those in the original system. Although the mass of each particle increases by a factor of $S_f^3$, the total number of particles decreases by the same factor, conserving total mass throughout the simulation.

Bierwisch et al. [35] also demonstrated that energy dissipation per volume and time is preserved when the coefficient of restitution remains unchanged, allowing kinetic energy density to be retained since particle velocities are unaffected by scaling. This strategy enabled us to achieve significant computational efficiency while maintaining a level of accuracy consistent with real tests. The scaling factor for the particles of both powders was 6 in this study.

Table 4 demonstrates the material properties considered in the simulations for modeling the two powders.

The filling mass presented in Table 3 corresponds to the values utilized in the majority of the simulations. In the simulations where a mass of 4 kg was employed, the number of particles was doubled. The time step was defined to ensure that it consistently represents less than 20 % of the Rayleigh time. The corresponding equation is defined as follows:

**Table 3**
DEM input parameters for both powders.

| Material parameter/contact model | Symbol | Unit | SpheroLac 100 | Ascorbic Acid |
|---|---|---|---|---|
| Young's modulus | $Y_F$ | GPa | 0.026 | 0.026 |
| Poisson's ratio | $\nu$ | | 0.3 | 0.3 |
| Particle diameter (after coarse-graining) | $d_p$ | μm | 690 | 253.2 |
| Contact law parameters | | | | |
| Coefficient of restitution particle-particle | $e_{pp}$ | | 0.17 | 0.2 |
| Coefficient of restitution particle-wall | $e_{pw}$ | | 0.17 | 0.2 |
| Coefficient of static friction particle-particle | $\mu_{s,pp}$ | | 0.6 | 0.473 |
| Coefficient of static friction particle-wall | $\mu_{s,pw}$ | | 0.4 | 0.368 |
| Coefficient of rolling friction particle-particle | $\mu_{r,pp}$ | | 0.2 | 0.14 |
| Coefficient of rolling friction particle-wall | $\mu_{r,pw}$ | | 0.15 | 0.12 |
| Cohesion Energy Density | $C_{pw}$ | $J/m^3$ | 4000 | 200,000 |
| Factory settings | | | | |
| Filling mass | | g | 1980 | 20 |
| Number of particles | | | $9.14 \times 10^6$ | $7.03 \times 10^3$ |
| Acceleration due to gravity | $g$ | $m/s^2$ | 9.81 | 9.81 |
| Simulation time step | | s | $1.39 \times 10^{-6}$ | |

$$\mathbf{T_R} = \frac{\pi R\sqrt{\frac{\rho}{G}}}{0.1631\nu + 0.8766} \tag{2}$$

This approach guarantees stability in the simulations while capturing the essential dynamics of the mixing process.

### 2.3. Mixing quality analysis

#### 2.3.1. Mixer experimental setup

The mixing experiments were conducted inside a stainless-steel mixing chamber of conical shape. The design and geometry of the mixer are illustrated in Fig. 1. The mixer is covered at the top and the bottom of the device. The cover at the bottom is conically shaped and remains closed during the filling and mixing process, after which is opened to let the mixed powders flow out of the device.

In the upper cover, products are fed into the device though two holes connected to Brabender screw feeders at the top cover, and the mixing process is achieved by rotating a stirrer connected directly to a motor. In the experiments, an initial loading arrangement was considered in which the active pharmaceutical ingredient (API) was sandwiched between layers of SperoLac 100 as a trial method. However, this approach was not continued, as no significant difference in mixing behavior was observed when both powders were fed simultaneously. Since feeding the two powders simultaneously proved to be more efficient and faster in practical applications, this method was adopted as the sole approach in the study. This decision allowed the mixing process to be streamlined while still ensuring effective interaction between the components. All the process parameters including the stirrer rotational speed, fill level of the products, feeding behavior and the mixing duration are assigned via a display screen with a user-friendly interface.

The performance of different stirrers shown in Fig. 2 was investigated and compared in this study in order to obtain the design with the optimal mixing degree.

#### 2.3.2. Mixing degree in simulations

The geometry of the mixing stirrer used in this study does not allow the particles to be always existing in the same region of the mixer all through the experiments. For that, the mixing region was completely discretized in 3D into equally divided small volumes. After which, all the particles were tracked in terms of the number positioned inside each of these volumes. The quantification of mixing was based on the relative number of particles existing in each of the discretized cells. In this study, the term "mixing degree" is defined for representing the mixing quality. At each time step, the mixing degree is calculated according to the following equation:

$$\mathbf{m} = \mathbf{1} - \frac{|\mathbf{Cn_2} - \mathbf{n_1}|}{\mathbf{Cn_2} + \mathbf{n_1}} \tag{3}$$

where $m$ is the mixing degree, $n_2$ and $n_1$ are the number of particles of powders of type 2 and type 1 respectively and C is the ratio between

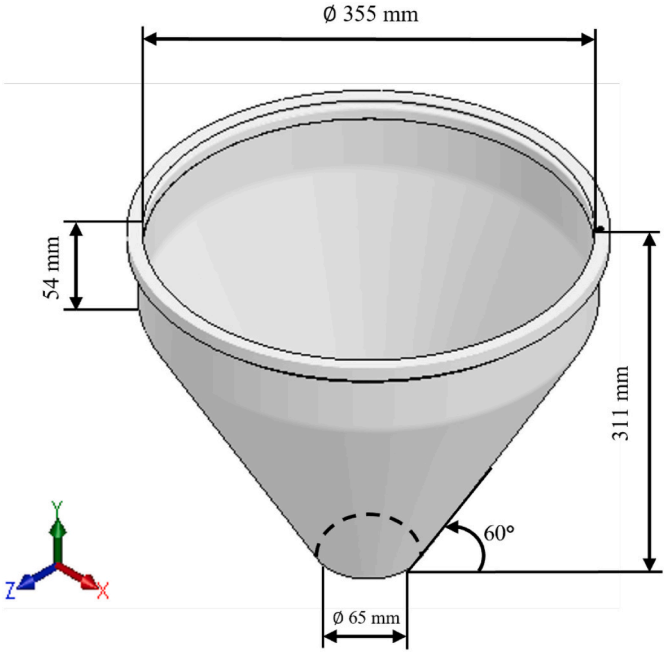


**Fig. 1.** Illustration of the mixing container used in the experiments.

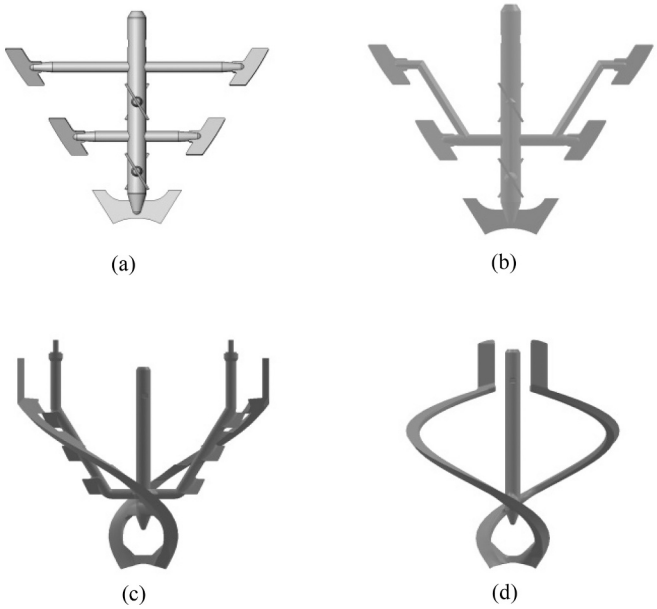


**Fig. 2.** Designs of the different stirrers used in the simulations namely, (a) Paddle, (b) Modified Paddle, (c) Rotor-Stator, and (d) Spiral.

particles 1 and 2. Based on this equation, the mixing degree is indeed calculated for each of the small volumes (cells). Afterward, a single value representing the overall mixing degree of the entire tank is obtained by averaging the mixing degree values from all the cells. As the mixing degree approaches the value of 1 a perfect mix is indicated.

On the other hand, the experiments show that in some cases the mixing quality is significantly heterogeneous within the mixing chamber. Thus, the mixing degree calculated inside the small cells is shown with a color scale in the mixer volume in order to infer the difference mixing zones, Fig. 3. This approach allows us to evaluate the mixing degree locally in specific regions of the chamber, providing a more detailed and localized assessment of the mixing behavior.

The size of these bins is very critical, as it can significantly influence the calculated degree of mixing. In our methodology, we adopted a systematic approach by progressively reducing the cell size until the final mixing degree no longer changed. This ensures that we obtain a reliable measurement. Additionally, we ensured that the cell volumes were sufficiently large to accommodate enough particles, allowing them to effectively represent the overall behavior of the mixture. The exact dimensions of these cells were 10 mm in both the length (z-direction) and width (x-direction), and 8 mm in height (y-direction).

#### 2.3.3. Experimental mixing qualification

The experimental quantification of the mixing quality was performed using the UV–Visible spectroscopy technique. The absorption of light is governed by Beer-Lambert law, which states that the absorbance of light is in direct relation to the path length of the absorbing medium and the number or concentration of absorbing molecules in the light path.

In this study, the Specord 200 plus (Analytik Jena GmbH, Germany) was utilized and ten samples from ten different levels in the horizontal axis were extracted after the mixing process was finished. The objective of this production line unit is to achieve continuous mixing and outfilling. For that, after completing the mixing process, the lower cover of the mixing chamber was opened—reflecting actual operational procedures—allowing collect ten samples from ten different levels along the horizontal axis at ten distinct time steps. Each sample represents a section of the mixture at various levels within the mixing chamber, capturing the dynamic nature of the mixing process. The goal was to detect the concentration of one of the powders, referred to as reference powder, in each of the samples. Therefore, 1 g of sample was taken and dissolved in 1 l of distilled water individually. Then, sample solutions from each were taken in absorption cells or cuvettes and were exposed to light beam from the light source. The broadband light beam is resolved into individual wavelengths by the monochromator and the isolated wavelengths are led to the sample in a sequence called scanning. The absorbing species absorb selectively, and the absorbance (A) is plotted as ordinate against the wavelength (λ) as abscissa. The resulting plot is called a spectrum. The wavelength of maximum absorbance is important and referred to as A max which is selected to calculate the concentration of the reference powder.

After the maximum absorption for each sample was detected, the relative standard deviation (RSD) of all these values was calculated, a lower value of which is directly linked to a more homogeneous mixture and consequently a better mixing performance.

## 3. Results

In the field of powder mixing, several factors can play a major role in influencing the mixing quality. Some of these factors belong to the design of the devices used in experiments and some to the material itself. In this study, a broad and intensive investigation was done to check how changing the geometry and some material characteristics would affect the mixing behavior. The results can be considered as a reference for the setup of further experiments.

### 3.1. Geometry

The influence of stirrer geometry on the overall mixing index is outlined in Table 4 for different particle mass loads. As it can be seen, the Paddle (PA), Modified Paddle (MPA), and Rotor-Stator (RS) showed the best results with comparatively similar mixing indexes for both 2 kg and 4 kg, while the Spiral (SP) geometry showed significantly worse mixing performance. Given that the PA geometry shows marginally better results for 2 kg, this geometry has been used for the analysis of the remaining factors.

In order to validate the capacity of the numerical model to predict mixing behavior, mixing processes using different stirrers were also performed, after which experimental qualification for the obtained mixtures was conducted. Since the simulations showed almost no difference in terms of mixing degree upon mixing 4 kg using different

**Table 4**
Change of the mixing degree under two solid loads and each of the stirrer designs.

| Mass (kg) \ Geometry | Paddle | Modified Paddle | Rotor-Stator | Spiral |
|---|---|---|---|---|
| 2 | **0.76** | 0.71 | 0.73 | 0.5 |
| 4 | 0.81 | 0.81 | 0.81 | 0.56 |

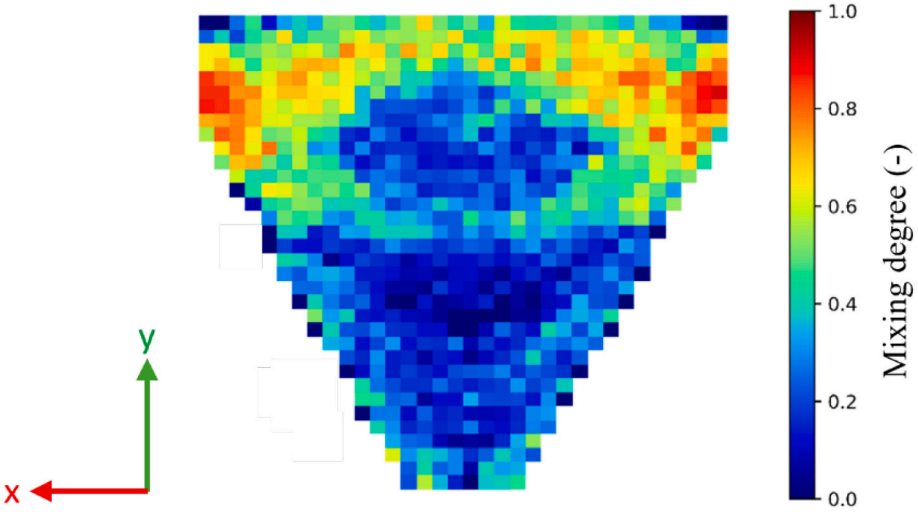


**Fig. 3.** Distribution of the particle mixing degree inside the mixer.

stirrers, only the 2 kg cases were considered in these experiments.

Every graph in the Fig. 4 includes ten plots for each of the ten samples extracted from each mixture. The plots represent the concentration of the reference powder in these samples. As explained in a previous section, the RSD of the maximum absorption values in each mixture is calculated and presented in Fig. 5.

It can be seen that the results from the experiments coincide with the results in the simulations. Both indicate that the PA, MPA, and RS stirrers are remarkably outperforming the SP stirrer with RSD values of 1.9, 3.2, 2.7, and 15.2 respectively. Moreover, the slight difference in the achieved mixing degree upon using PA, MPA, and RS was also observed in the experiments in the same order the simulations showed. From a performance perspective, not only the final mixing value is important, but also the time required to reach the final mixing state. Thus, as the three stirrers, i.e. PA, MPA, and RS are showing relatively close final results in terms of mixing quality, it was important to check the behavior of the mixing in the transient phase and make a comparison in Fig. 6.

As it is shown, the development of the mixing degree throughout the simulations using the four stirrers widely varies depending on which device is employed. Especially in the transient phase before reaching the steady state of mixing, where the SP stirrer results in the worst steady state mixing degree but curiously enough, it is also the one with the fastest mixing degree growth. On the other hand, it can be also indicated that the RS stirrer requires longer time to reach the steady state in comparison to the PA and MPA, which are showing similar behavior with a slight outperformance of MPA over the PA. Still, the PA was considered to be more adequate for our studied cases for two reasons. First, the fabrication of MPA is more expensive due to some additional complexity in the design. Second, the sharp angles of the arms of the stirrer are causing residuals at the end of the mixing process leading to no homogeneity in upper layer of the mixture. For more clarity, Fig. 7 was developed to show the difference in the behavior of the mixtures upon using the four stirrers in terms of mixing degree distribution.

Fig. 7 shows the distribution of the mixing degree inside the mixer. It indicates the parts of the mixer having a good mixing quality and the ones having bad mixing according to the scale represented. Fig. 7(d) clearly indicates how bad the mixing behavior using the SP stirrer is. Moreover, looking at Fig. 7(b) and Fig. 7(c), the mixtures obtained using the MPA and RS stirrers are having a layer at the top, which is not being well mixed. This is due to the presence of remarkable amount of the lower density powder on the top of the mixture. In addition, the design of these two stirrers allows more residuals to remain sticking on their axes and blades until the end of the mixing process, after which they fall without being well mixed. Especially upon using the RS, which is showing a slightly better performance over the MPA in terms of mixing degree. This indicates that choosing the optimal stirrer should not be based on the mixing degree only, rather all the circumstances of the process line should be taken into consideration. Fig. 7(a) shows how the region is filled with the red areas the most. On the other hand, comparing Fig. 7(a) and Fig. 7(b) points out to a difference in terms of compaction of the mixtures. Using the PA stirrer is leading to a convex top, whereas using the MPA is leading to a concave top of the mixture. This shows how the design of the stirrers has an influence on the void fraction of the particles and that a better mixing degree is obtained as the mixture is more compacted. A clear correlation between porosity and the mixing degree was observed in the study. Specifically, it was found that lower porosity corresponds to more compacted particles, which is essential for achieving better mixing. This relationship was consistently demonstrated across the various simulations, highlighting the


**Fig. 5.** Experimental relative standard deviation of the maximum absorption values referring to the mixing qualities.

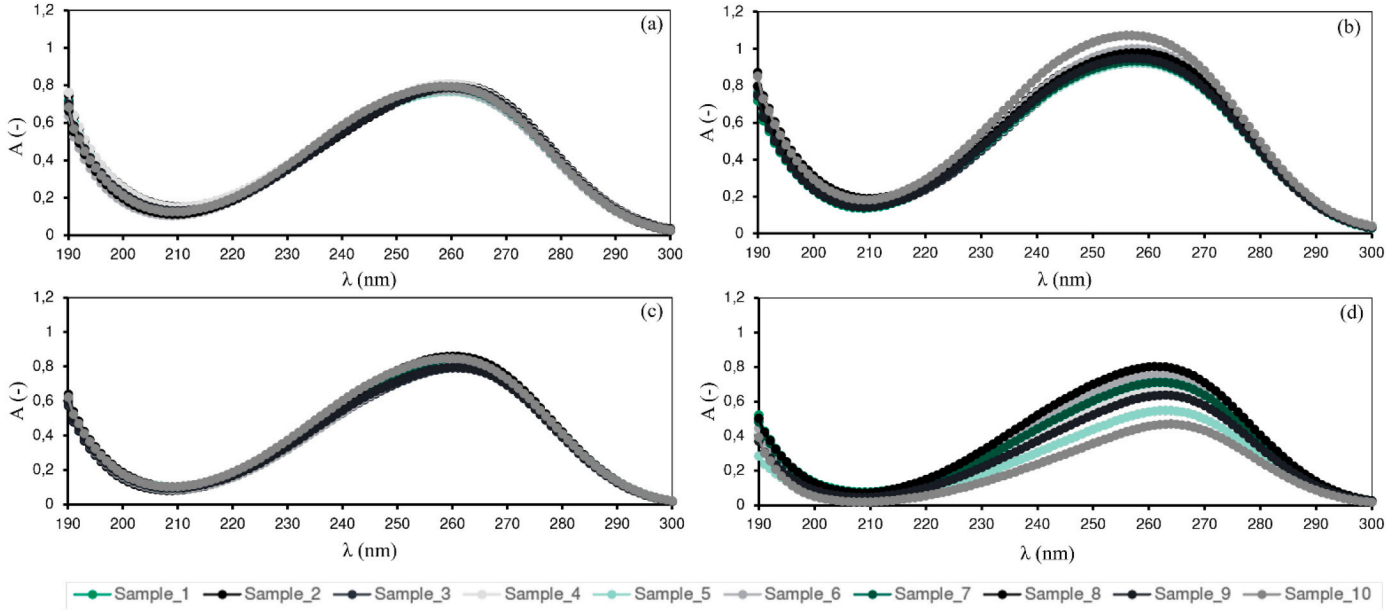


**Fig. 4.** Absorption values in terms of the wavelength of the light issued by the UV/Vis device for samples of mixtures obtained using (a) PA, (b) MPA, (c) RS, and (d) SP Stirrers.

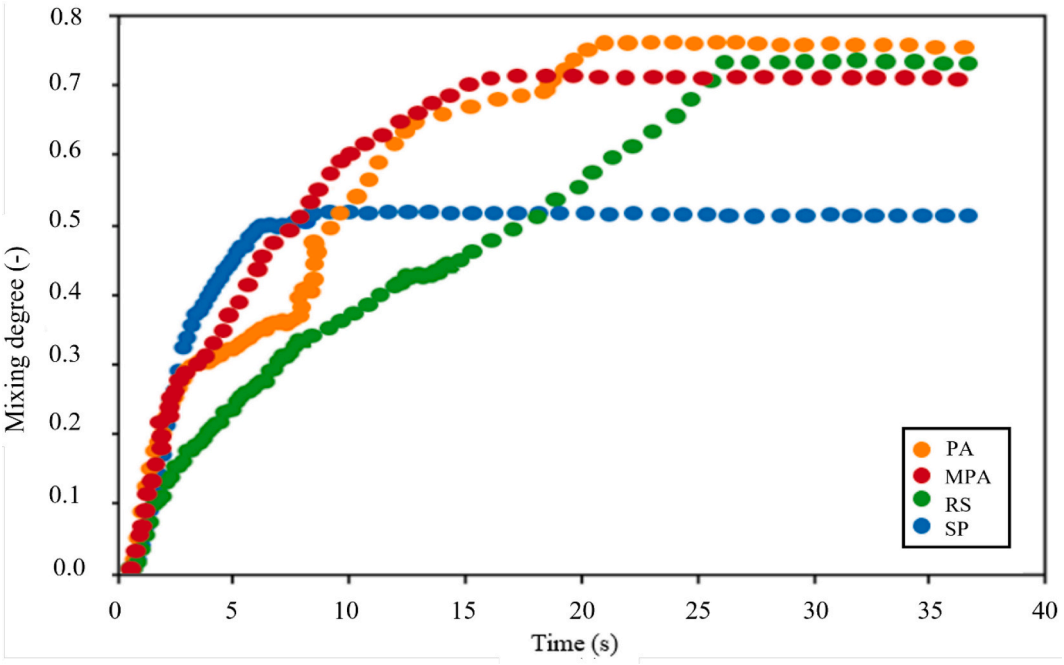


**Fig. 6.** Temporal behavior of the mixing degree using different stirrers.

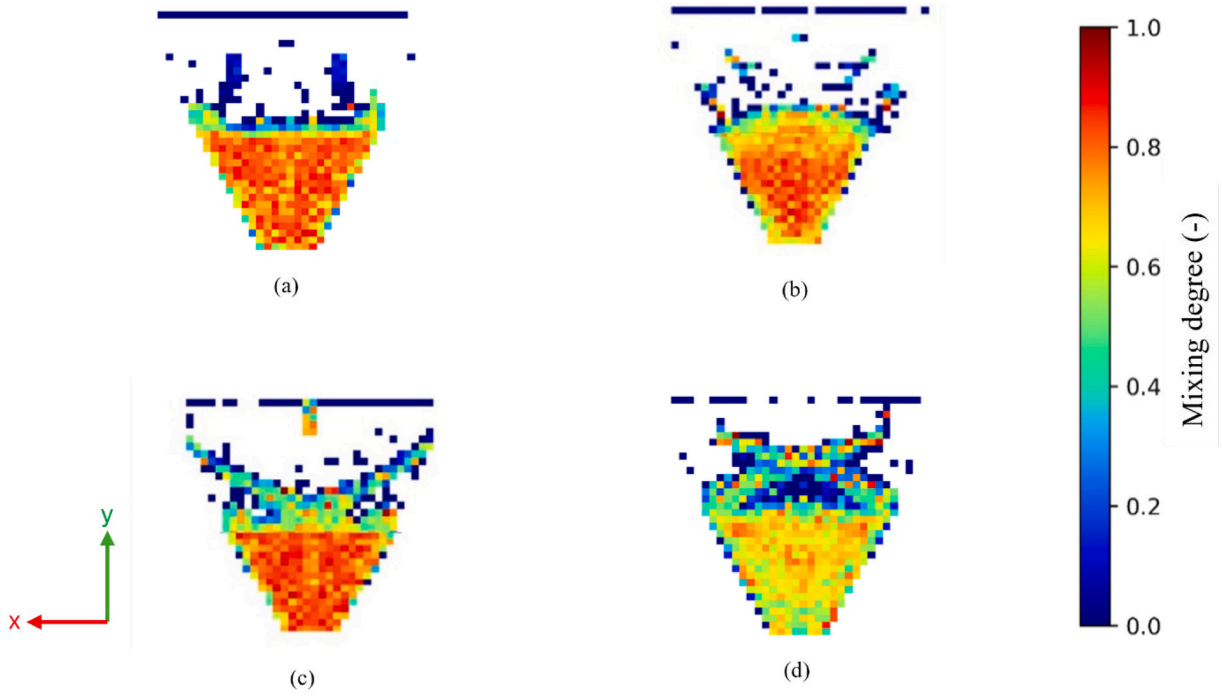


**Fig. 7.** Mixing degree distribution inside the mixing chamber upon using (a) PA, (b) MPA, (c) RS, and (d) SP stirrers.

importance of particle arrangement in the overall mixing process. The porosity ($\epsilon$) of each of the four mixtures was calculated according the following equation:

$$\epsilon = 1 - \frac{BD}{\rho_p} \times 100\% \quad (4)$$

The corresponding results are listed in Table 5.

Fig. 7 proves the superiority of the PA stirrer over the other three stirrers not only in terms of mixing degree, but also in terms of the homogeneity of the particles all through the mixing container.

**Table 5**
The porosity of the mixtures using different stirrers.

| Geometry | Paddle | Modified Paddle | Rotor-Stator | Spiral |
|---|---|---|---|---|
| $\varepsilon$ (%) | 0.44 | 0.5 | 0.48 | 0.55 |

### 3.2. Parametric study

Apart from the aforementioned stirrer design, the mixing index could also be affected by other factors, such as rotation speed, filling ratio, and

particle density. Thus, these three parameters were studied and their effect on the mixing index was inferred. The maximum stirring speed available for the experiments is 500 rpm. Thus, values representing low, medium, and high stirring speeds were selected, namely 100, 250, and 400 rpm respectively. Fig. 8 (a) shows that an increase in the rotation speed progressively improves the mixing index. The slopes for both lines are quite similar, resulting from a similar influence of the rotational speed, regardless of the amount of material under study. Still, it can also be seen that at every stirring speed a higher amount of material improves the solid mixing. The reason for that is a more effective transfer of momentum from the blades to the particles and, through frictional interactions, from these particles to their neighbors as the container is fully filled. These interactions contribute to letting the particles of the mixed materials interfere.

It has been observed that at high rotational speeds, particles remain at the upper part of the mixer, while at low rotational speeds particles remain at the bottom. Therefore, an intermittent regime has been implemented, where the rotational speed is switched between 400 and 100-400 rpm in order to keep particles well mixed. The total duration of the mixing process was 1 min, with speed changes occurring at specific intervals. The process began at 400 rpm for the first 20 s to ensure effective initial mixing and particle distribution. After this, the speed was reduced to 100 rpm for the next 20 s, promoting more uniform mixing by allowing particles to settle slightly, enhancing the overall mixing degree during this phase. For the final 20 s, the speed was increased back to 400 rpm to re-energize the mixing process, effectively re-suspending and thoroughly mixing any settled particles.

This intermittent speed variation was designed to create a shaking effect, promoting vertical movement of the mixture, allowing particles to flow up and down and improving their interaction within the chamber. These transitions occurred automatically according to predefined settings in the Human-Machine Interface (HMI) of the machine, offering flexibility in adjusting the parameters to suit different mixing scenarios. This phenomenon, as shown in Fig. 8 (a), proves to improve the mixing index regardless of the bed mass, even though a higher solid inventory is still preferable.

One of the major problems regarding the mixing processes in the industrial field is that the mixers are not able to give the same mixing quality with different ratios of the amount of the materials to be mixed. In order to check the flexibility of the mixer with varying ratios of the material, three different percentages were used, i.e. 1, 10, and 50 %. On the one hand, it has been shown, that the best mixing degree was attained while using the same amount of each material (50 %). The case of 1 % ratio has shown to mix very poorly and require further modifications that will be explained in the coming section. Fig. 8 (b) shows that changing the amount ratio from 1 % to 10 % had a modest effect on the mixing degree with 4 kg mass, whereas it clearly improved the mixing index for the case of 2 kg mass. Once the ratio was changed from 10 % to 50 %, the enhancement of the mixing degree with 4 kg was much stronger and reached the highest mixing degree. Moreover, it can be also be observed that at a certain ratio, the same mixing degree is attained, which indicates that considering some interactions can let the ratio does not influence the final mixing quality.

As the density of the powder affects the movement of its particles during transportation, other density ratios (DR) were considered while keeping the same ratio of the size of particles between the mixed powders. Fig. 8 (c) is designed to show the efficiency of varying the rotational speed of the stirrer while considering different DR. It can be seen that varying the rotational speed has a greater influence the larger the difference between the particle densities is, as constant stirring velocity might result in particle segregation. Thus, no constant speeds should be used with mixtures that are prone to segregate.

### 3.3. Deflector and cohesivity

Although the mixing degree was improved by varying the rotational speed within the mixing process, particles still collide with the top cover at 400 rpm. Due to the design of the PA stirrer, the material is forced to the wall through centrifugal force, which results in an axial region with lower amounts of powder, as shown in Fig. 9.

This becomes problematic when trying to feed new material in the mixer as the top inlets become clogged. Therefore, particles need to be moved from the top of the mixer to the bottom without, preferably, touching the top cover. For that, several modifications, shown in Fig. 10, were done to the mixing blades, such as elongating the stirring blades Fig. 10(a), adding some bores to the design Fig. 10(b), and changing the position and angle of the stirring blades, Fig. 10(c). However, none of these modifications accomplished the desired result as where able to accumulate on the mixer wall.

After that, it was thought to keep the design of the stirrer without modifications and to assemble another component, i.e. deflector, to the mixer itself, so that the particles must be forced to transfer from the wall to the center, with the aim of enhancing the solid mixing and increasing the overall volume utilization through this solid circulation. Thus, to accomplish the homogenization of the solid fraction field, a number of deflectors have been designed and built, namely U-Shape, curved, and fork deflector, Fig. 11.

Firstly, the U-Shape deflector was used and located at the upper section of the mixer as shown in Fig. 12. As shown from the solid distribution, the addition of this passive device results in a significant improvement of the particle dispersion throughout the container. Thus, these new deflectors are explored with the original design of the PA stirrer.

As the mixing of 4 kg already showed the best quality the mixture can reach, the focus was concentrated on interpreting the mixing behavior with 2 kg. It can be seen that with lower masses, using a three-phase speed scheme is showing a clear improvement in the mixing quality in comparison to using one constant speed. This effect was considered to be more modest with higher masses. The reason for that is that this method is based on having somehow a circular motion of the particles in the vessel, which leads to an increase in the homogeneity of the mixture due to the increase in the interactions between the particles all through the mixing region. But, upon feeding 4 kg in the mixer, the mixing chamber is almost full. By that, the movement of the particles is not that much flexible as with 2 kg because they are not having enough free space to move in freely as in the first case.

The modeled powders in the simulations so far were already cohesive, but since a lot of materials involved in the industrial field are much more cohesive, the effects of all previously implemented modifications were examined with higher cohesivity value.

Fig. 13 shows that each modification played a role in enhancing the mixing quality, especially using the fork design of the deflector. The fork was designed in this shape in order to split the particles that are accumulating with each other due to the cohesivity of the material. As the cohesion values defined in the initial set-up of the the simulations are considered not to be high, this design showed no improvement in the mixing quality. But as the assigned cohesivity was increased, the fork has proved to be very efficient in such cases. Fig. 13 indicates that the properties of the materials involved in such experiments can conspicuously influence the mixing behavior. Therefore, both the design of the mixer along with the type of the powders should be taken into consideration in order to get the best-requisitioned mixing quality.

## 4. Conclusions

In the presented paper, a mixing process was modeled using DEM under different conditions. In order to quantify the mixing quality, a self-developed numerical method was used. The method has proved to be efficient in terms of the time of calculation and accuracy. The credibility of the suggested method has been verified via comparison with another accountable method in previous literature. The method offers several important advantages. One of the key strengths lies in its broad

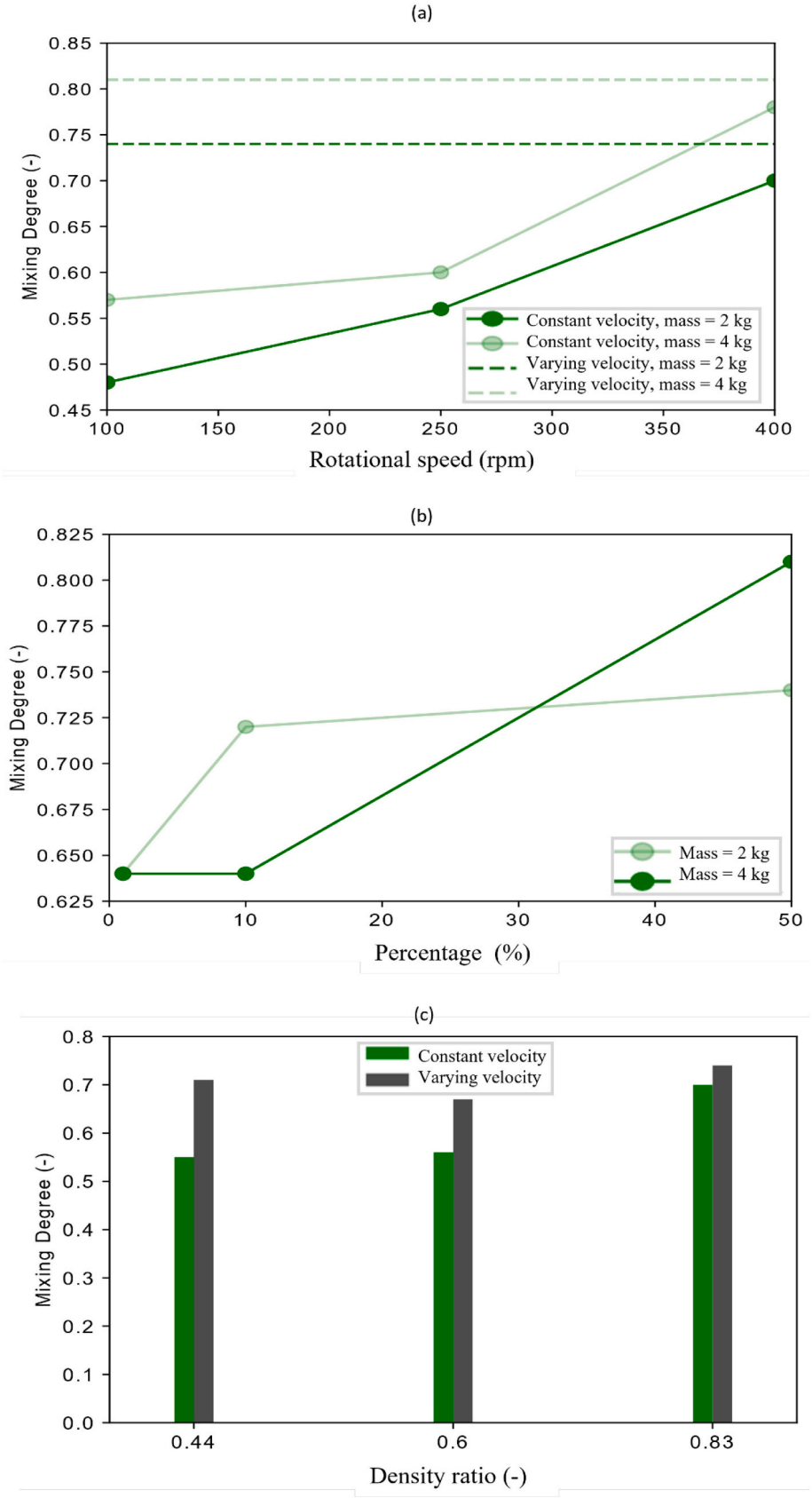


**Fig. 8.** Evolution of mixing degree by changing the (a) rotational speed, (b) filling ratio, and the (c) particle density ratio.

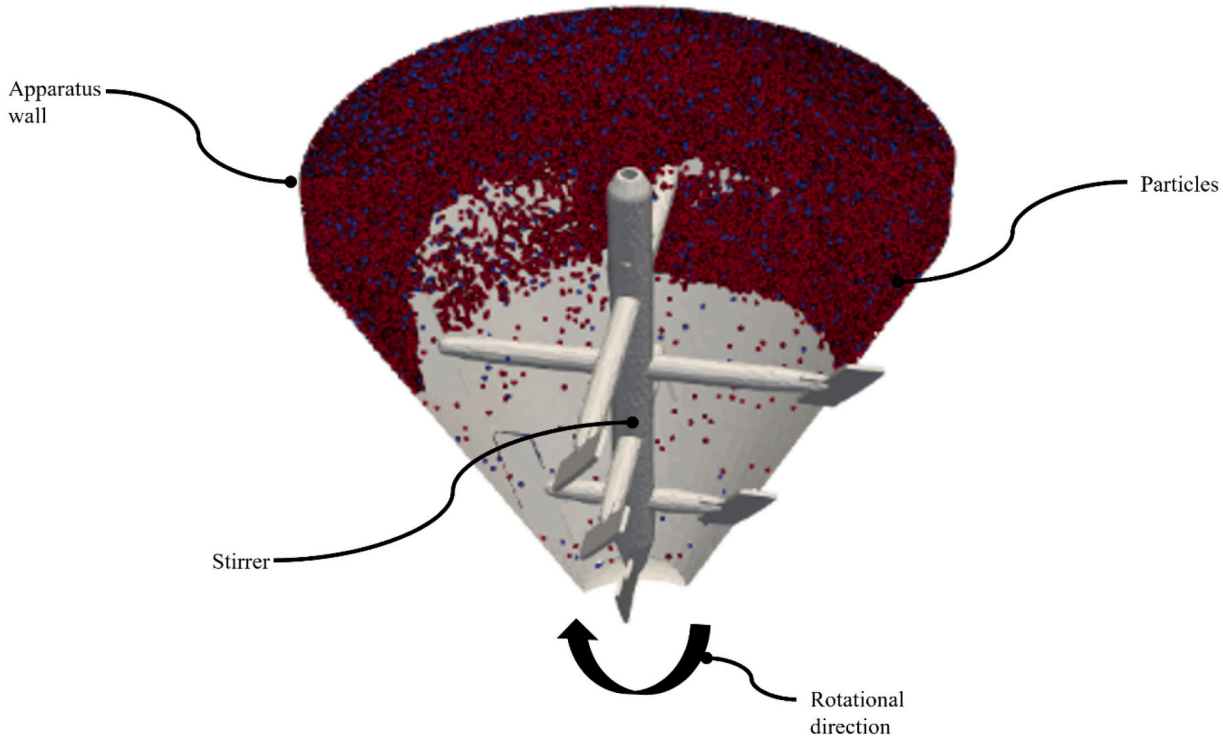


**Fig. 9.** The steadily positioning of the particles at the top of the mixer with PA stirrer.

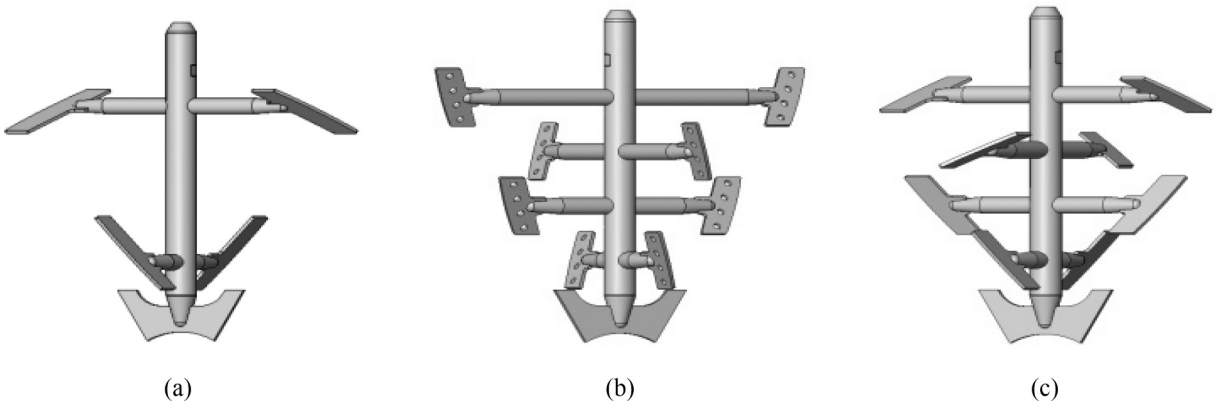


**Fig. 10.** Modifications applied to the PA stirrer represented by (a) removing the middle sub axes and elongating the remaining blades, (b) applying bores to the blades, and (c) changing the angular positions of the blades.

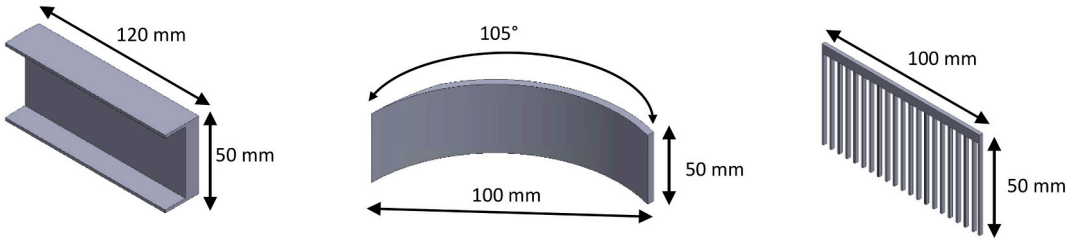


**Fig. 11.** Representation of (a) U-Shape, (b) Curved and (c) fork deflector design.

applicability, as it can be applied to all designs and boundary conditions. By accounting for all particles within the mixing tank, regardless of their positions, it provides a more comprehensive and accurate representation of the mixing process. This overcomes the limitations of other techniques, such as contact statistics and uniform distribution, which are restricted to situations where particles remain within a specific region defined by the user.

Another benefit is the simplicity of the formula, which allows for faster computation without compromising accuracy. This efficiency is crucial when working with large datasets or complex simulations,

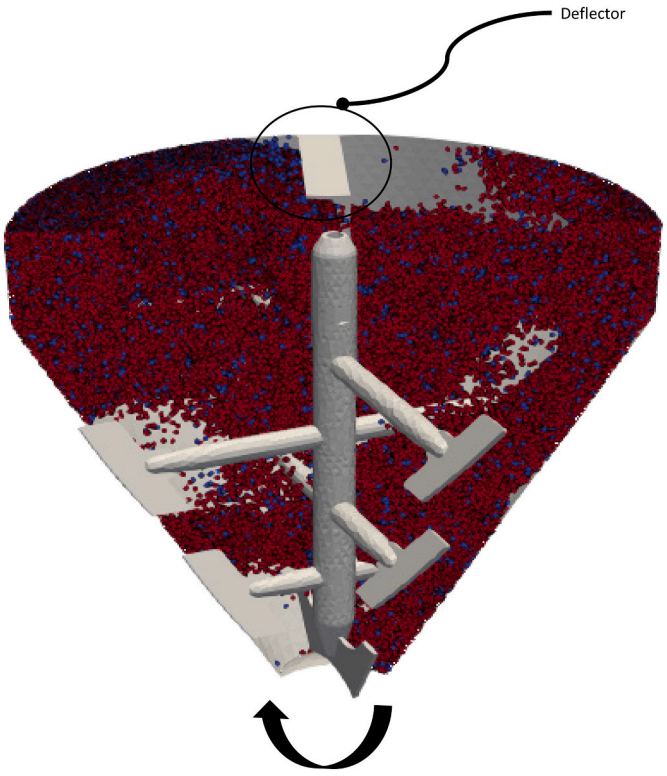


**Fig. 12.** Behavior of the particles after a deflector is assembled in the mixer.

reducing overall processing time. Furthermore, the method enables the quantification of the mixing degree locally, through detailed post-processing and visualization techniques. This allows us to assess the mixing behavior in specific regions of the chamber, providing deeper insights into areas of poor mixing or opportunities for optimizing design parameters.

Based on that, the influence of the stirrer design, stirrer rotational speed, powder density, cohesivity, materials ratios, and particle movement in the chamber guided through different designs of deflectors on the final mixing degree is examined and the following conclusions were drawn:

The rotating speed of the stirrer is a main factor affecting the mixing quality, where increasing the speed increases the mixing degree. Still, this effect becomes more significant with higher filling levels. Moreover, switching between high and low rotational speed within the single mixing process outperforms using one unique speed, especially for mixtures of solid with high relative densities. Increasing the transfer of momentum in the system, represented by additional interactions between the particles and the blades of the stirrer improves the final mixing degree.

Interchanging the position of the particles between the top and the bottom of the mixer through a deflector played a major role in enhancing the mixing quality specifically with more cohesive powders. Firstly, using this technique removes any obstacle to further feeding caused by an obstruction on the inlet of the mixing chamber. Additionally, the importance of this interchange can be more significant upon using the 3-phase speed scheme with lower masses.

The initial setup of the system is not flexible in terms of changing the ratio of the mixed materials. This issue can be overcome by implementing the deflector along with using the 3-speed scheme. It was shown that the mixing behavior is influenced by several factors in terms of boundary conditions and particle properties. The interactions between these factors in some cases are having more significant consequences. Thus, some sort of correlations should be considered in order to get the best mixing performance. These correlations should be based on the obtained results in this study according to the type of material to be used.

## CRediT authorship contribution statement

**Nizar Salloum:** Writing – original draft, Visualization, Validation, Software, Methodology, Conceptualization. **Thomas Brinz:** Writing – review & editing, Supervision, Formal analysis, Data curation. **Aitor Atxutegi:** Writing – review & editing, Visualization, Investigation. **Stefan Heinrich:** Writing – review & editing, Visualization,

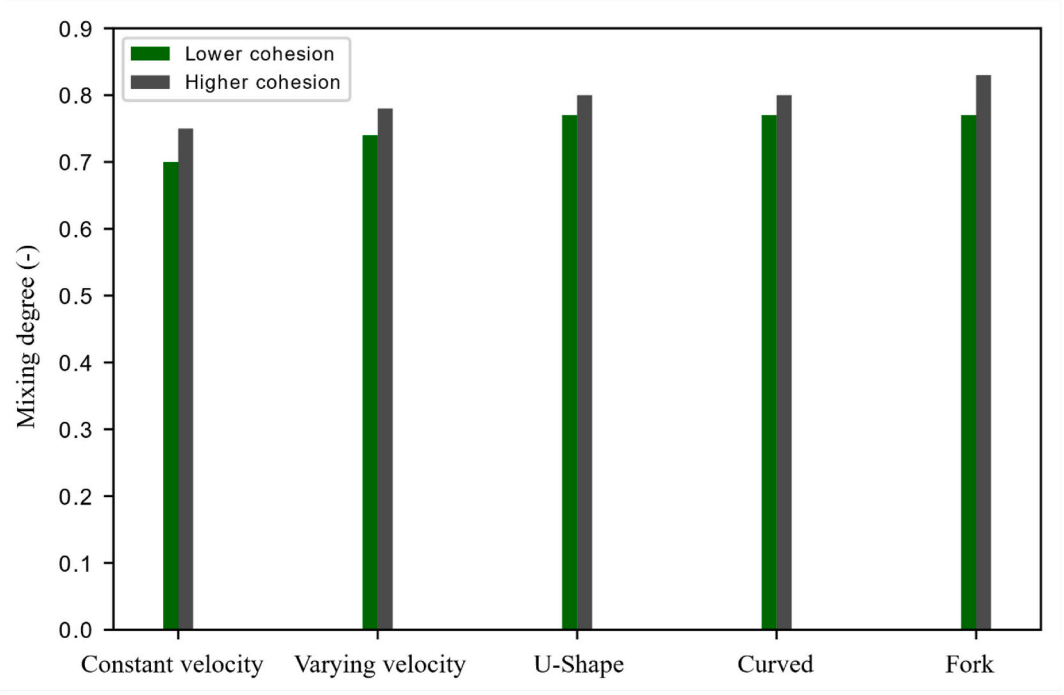


**Fig. 13.** Influence of velocity modes and deflector design in the overall mixing degree for powders of different cohesivities.

Investigation.

## Declaration of competing interest

The authors declare that they have no known competing financial interests or personal relationships that could have appeared to influence the work reported in this paper.

## Acknowledgements

This research did not receive any specific grant from funding agencies in the public, commercial, or not-for-profit sectors.

## Data availability

No data was used for the research described in the article.

## References

[1] I. Gijón-Arreortúa, A. Tecante, Mixing time and power consumption during blending of cohesive food powders with a horizontal helical double-ribbon impeller, J. Food Eng. 149 (2015) 144–152, https://doi.org/10.1016/j.jfoodeng.2014.10.013.
[2] A. Aït Aissa, C. Duchesne, D. Rodrigue, Polymer powders mixing part I: mixing characterization in rotating cylinders, Chem. Eng. Sci. 65 (2010) 786–795, https://doi.org/10.1016/j.ces.2009.09.031.
[3] P. Shenoy, E. Xanthakis, F. Innings, C. Jonsson, J. Fitzpatrick, L. Ahrné, Dry mixing of food powders: effect of water content and composition on mixture quality of binary mixtures, J. Food Eng. 149 (2015) 229–236, https://doi.org/10.1016/j.jfoodeng.2014.10.019.
[4] W. Shi, E. Galella, O. Sprockel, Macro- and micro-mixing of a cohesive pharmaceutical powder during scale up, Powder Technol. 274 (2015) 319–323, https://doi.org/10.1016/j.powtec.2015.01.049.
[5] A.A. Aissa, C. Duchesne, D. Rodrigue, Effect of friction coefficient and density on mixing particles in the rolling regime, Powder Technol. 212 (2011) 340–347, https://doi.org/10.1016/j.powtec.2011.06.009.
[6] R. Liu, X. Yin, H. Li, Q. Shao, P. York, Y. He, T. Xiao, J. Zhang, Visualization and quantitative profiling of mixing and segregation of granules using synchrotron radiation X-ray microtomography and three dimensional reconstruction, Int. J. Pharm. 445 (2013) 125–133, https://doi.org/10.1016/j.ijpharm.2013.02.010.
[7] J.G. Rosas, M. Blanco, A criterion for assessing homogeneity distribution in hyperspectral images. Part 1: homogeneity index bases and blending processes, J. Pharm. Biomed. Anal. 70 (2012) 680–690, https://doi.org/10.1016/j.jpba.2012.06.036.
[8] F.J. Muzzio, P. Robinson, C. Wightman, Dean Brone, sampling practices in powder blending, Int. J. Pharm. 155 (1997) 153–178, https://doi.org/10.1016/S0378-5173(97)04865-5.
[9] Y. Mori, M. Sakai, Advanced DEM simulation on powder mixing for ellipsoidal particles in an industrial mixer, Chem. Eng. J. 429 (2022), https://doi.org/10.1016/j.cej.2021.132415.
[10] X. Bednarek, S. Martin, A. Ndiaye, V. Peres, O. Bonnefoy, Extrapolation of DEM simulations to large time scale application to the mixing of powder in a conical screw mixer, Chem. Eng. Sci. 197 (2019) 223–234, https://doi.org/10.1016/j.ces.2018.12.022.
[11] M. Pezo, L. Pezo, A. Jovanović, B. Lončar, R. Čolović, DEM/CFD approach for modeling granular flow in the revolving static mixer, Chem. Eng. Res. Des. 109 (2016) 317–326, https://doi.org/10.1016/j.cherd.2016.02.003.
[12] M. Marigo, D.L. Cairns, M. Davies, A. Ingram, E.H. Stitt, Developing mechanistic understanding of granular behaviour in complex moving geometry using the discrete element method. Part B: investigation of flow and mixing in the Turbula® mixer, Powder Technol. 212 (2011) 17–24, https://doi.org/10.1016/j.powtec.2011.04.009.
[13] Q.F. Hou, K.J. Dong, A.B. Yu, DEM study of the flow of cohesive particles in a screw feeder, Powder Technol. 256 (2014) 529–539, https://doi.org/10.1016/j.powtec.2014.01.062.
[14] L. Pezo, A. Jovanović, M. Pezo, R. Čolović, B. Lončar, Modified screw conveyor-mixers - discrete element modeling approach, Adv. Powder Technol. 26 (2015) 1391–1399, https://doi.org/10.1016/j.apt.2015.07.016.
[15] P.Y. Liu, R.Y. Yang, A.B. Yu, DEM study of the transverse mixing of wet particles in rotating drums, Chem. Eng. Sci. 86 (2013) 99–107, https://doi.org/10.1016/j.ces.2012.06.015.
[16] R.Y. Yang, A.B. Yu, L. McElroy, J. Bao, Numerical simulation of particle dynamics in different flow regimes in a rotating drum, 9th international conference on bulk materials storage, handling and transportation, ICBMH 188 (2007) 170–177.
[17] B.K. Mishra, C. Thornton, D. Bhimji, A preliminary numerical investigation of agglomeration in a rotary drum, Miner. Eng. 15 (2002) 27–33, https://doi.org/10.1016/S0892-6875(01)00194-7.
[18] M. Lemieux, F. Bertrand, J. Chaouki, P. Gosselin, Comparative study of the mixing of free-flowing particles in a V-blender and a bin-blender, Chem. Eng. Sci. 62 (2007) 1783–1802, https://doi.org/10.1016/j.ces.2006.12.012.
[19] M. Lemieux, G. Léonard, J. Doucet, L.A. Leclaire, F. Viens, J. Chaouki, F. Bertrand, Large-scale numerical investigation of solids mixing in a V-blender using the discrete element method, Powder Technol. 181 (2008) 205–216, https://doi.org/10.1016/j.powtec.2006.12.009.
[20] H.P. Kuo, P.C. Knight, D.J. Parker, Y. Tsuji, M.J. Adams, J.P.K. Seville, The influence of DEM simulation parameters on the particle behaviour in a V-mixer, Chem. Eng. Sci. 57 (2002) 3621–3638, https://doi.org/10.1016/S0009-2509(02)00086-6.
[21] S. Golshan, R. Zarghami, H.R. Norouzi, N. Mostoufi, Granular mixing in nauta blenders, Powder Technol. 305 (2017) 279–288, https://doi.org/10.1016/j.powtec.2016.09.059.
[22] Y. Tsugeno, M. Sakai, S. Yamazaki, T. Nishinomiya, DEM simulation for optimal design of powder mixing in a ribbon mixer, Adv. Powder Technol. 32 (2021) 1735–1749, https://doi.org/10.1016/j.apt.2021.03.026.
[23] S. Pantaleev, S. Yordanova, A. Janda, M. Marigo, J.Y. Ooi, An experimentally validated dem study of powder mixing in a paddle blade mixer, Powder Technol. 311 (2017) 287–302, https://doi.org/10.1016/j.powtec.2016.12.053.
[24] Z. Zhang, L. Wang, Y. Wang, X. Chu, Discrete element simulation on mixing of granular materials in rotated container, Eng. Anal. Bound. Elem. 106 (2019) 20–26, https://doi.org/10.1016/j.enganabound.2019.04.034.
[25] S.H. Chou, Y. Lou Song, S.S. Hsiau, A study of the mixing index in solid particles, Kona Powder Part. J. 2017 (2017) 275–281, https://doi.org/10.14356/kona.2017018.
[26] F. Geng, Y. Wang, Y. Li, L. Yuan, X. Wang, M. Liu, Z. Yuan, Numerical simulation on mixing dynamics of flexible filamentous particles in the transverse section of a rotary drum, Particuology 11 (2013) 594–600, https://doi.org/10.1016/j.partic.2012.07.007.
[27] D.R. Van Puyvelde, Comparison of discrete elemental modelling to experimental data regarding mixing of solids in the transverse direction of a rotating kiln, Chem. Eng. Sci. 61 (2006) 4462–4465, https://doi.org/10.1016/j.ces.2006.02.013.
[28] X.Y. Liu, L. He, Comparison of image-based measuring methods for analysis of particle mixing in rotary drum, in: Lecture Notes in Electrical Engineering 212 LNEE, 2013, pp. 827–832, https://doi.org/10.1007/978-3-642-34531-9_88.
[29] S.-H. Chou, Y.-L. Song, S.-S. Hsiau, A study of the mixing index in solid particles, Kona Powder Part. J. 34 (2017) 275–281, https://doi.org/10.14356/kona.2017018.
[31] M. Yamamoto, S. Ishihara, J. Kano, Evaluation of particle density effect for mixing behavior in a rotating drum mixer by DEM simulation, Adv. Powder Technol. 27 (2016) 864–870, https://doi.org/10.1016/j.apt.2015.12.013.
[32] Meggle Excipients and Technology, Lactose Monohydrate USP/NF, EP, JP, IP. https://www.signetexcipients.com/product.aspx?prdid=13, 2024.
[33] A.C. Caritá, B. Fonseca-Santos, J.D. Shultz, B. Michniak-Kohn, M. Chorilli, G. R. Leonardi, Vitamin C: one compound, several uses, in: Advances for delivery, efficiency and stability, Nanomedicine: Nanotechnology, Biology, and Medicine 24, 2020, pp. 102–117, https://doi.org/10.1016/j.nano.2019.102117.
[34] B. El-Kassem, N. Salloum, T. Brinz, Y. Heider, B. Markert, A multivariate regression parametric study on DEM input parameters of free-flowing and cohesive powders with experimental data-based validation, Comput. Part. Mech. 8 (2021) 87–111, https://doi.org/10.1007/s40571-020-00315-8.
[35] C. Bierwisch, T. Kraft, H. Riedel, M. Moseler, Three-dimensional discrete element models for the granular statics and dynamics of powders in cavity filling, J. Mech. Phys. Solids 57 (2009) 10–31, https://doi.org/10.1016/j.jmps.2008.10.006.
[36] B. El Kassem, N. Salloum, T. Brinz, Y. Heider, B. Markert, A semi-automated DEM parameter calibration technique of powders based on different bulk responses extracted from auger dosing experiments, KONA Powder Part. J. 38 (2021) 235–250, https://doi.org/10.14356/kona.2021010.
[37] Z. Li, J. Yang, X. Xu, X. Xu, W. Yu, X. Yue, et al., Particle shape characterization of fluidized catalytic cracking catalyst powders using the mean value and distribution of shape factors, Adv. Powder Technol. 13 (2002) 249–263, https://doi.org/10.1163/156855202320252435.